Characterization of the Autoxidation of Terpenes at Elevated Temperature Using High-Resolution Mass Spectrometry: Formation of Ketohydroperoxides and Highly Oxidized Products from Limonene

Zahraa Dbouk, Nesrine Belhadj, Maxence Lailliau, Roland Benoit, Philippe Dagaut

Characterization of the Autoxidation of Terpenes at Elevated Temperature Using High Resolution Mass Spectrometry: Formation of Ketohydroperoxides and Highly Oxidized Products from Limonene.

Zahraa Dbouk[1,2], Nesrine Belhadj[1,2], Maxence Lailliau[1,2], Roland Benoit[1] and Philippe Dagaut[1,*]

[1]CNRS-INSIS, Institut de Combustion, Aérothermique, Réactivité, Environnement, Avenue de la recherche scientifique, 4507 Orléans, France

[2]Université d'Orléans, Avenue de Parc Floral, 45067 Orléans, France

Correspondence: dagaut@cnrs-orleans.fr

KEYWORDS: terpenes, limonene, autoxidation, high-resolution mass spectrometry, jet-stirred reactor

ABSTRACT: Low-temperature experiments on the oxidation of limonene-O_2-N_2 mixtures were conducted in a jet-stirred reactor (JSR) over a range of temperatures (520 to 800 K), fuel-lean conditions (equivalence ratio φ = 0.5), short residence time (1.5 s) and a pressure of 1 bar. Collected samples of the reacting mixtures were analyzed by (i) on-line Fourier transform infrared spectroscopy (FTIR) and (ii) Orbitrap Q-Exactive® high resolution mass spectrometry after direct injection or chromatographic separation using reversed-phase ultra-high-performance liquid chromatography (RP-UHPLC) and soft ionization (+/– heated electrospray ionization and +/– atmospheric pressure chemical ionization). H/D exchange using deuterated water (D_2O) and reaction with 2,4-dinitrophenylhydrazine (2,4-DNPH) were performed to probe the presence of OH, OOH and C=O groups in the oxidized products, respectively. A broad range of oxidation products ranging from water to highly oxygenated products, containing five and more O-atoms, was detected ($C_7H_{10}O_{4,5}$, $C_8H_{12}O_{2,4}$, $C_8H_{14}O_{2,4}$, $C_9H_{12}O$, $C_9H_{14}O_{1,3\text{-}5}$, $C_{10}H_{12}O_2$, $C_{10}H_{14}O_{1\text{-}9}$, $C_{10}H_{16}O_{2\text{-}5}$, and $C_{10}H_{18}O_6$). Mass spectrometry analyzes were only qualitative whereas quantification was performed with FTIR. The results are discussed in terms of reaction routes involving the initial formation of peroxy radicals, H-atom transfer and O_2 addition sequences producing a large set of chemical products among which ketohydroperoxides and more oxygenated products. Carbonyl compounds deriving from the Waddington oxidation mechanism on *exo*- and *endo*-double bonds (C=C) were observed as well as their products of further oxidation. Products of the Korcek mechanism (carboxylic acids and carbonyls) were also detected.

1. INTRODUCTION

Whereas terpenes are emitted by vegetation and represent an important fraction of volatile organic compounds (VOCs) observed in the troposphere,[1-2] these high-energy-density cyclic hydrocarbons are also considered as potential biojet fuels.[3-6] They could also be used as drop-in fuels for greener ground transportation since cetane numbers of ~ 20 have been reported[7]. The introduction of terpenes as fuel would contribute inevitably to increased emissions into the troposphere via unburnt fuel emissions and evaporation during, e.g., refueling. Although, the kinetics of oxidation of terpenes

under simulated tropospheric conditions has been extensively studied, a good knowledge of the numerous oxidation processes involved has not been reached.[8] Regarding the kinetics of combustion of this class of compounds, even less is known since, to our knowledge, only flame speeds and impact on ignition were studied.[9-12] While in atmospheric chemistry self-reactions and cross-reactions of peroxy radicals are of major importance,[13] in combustion[14-18] it is generally accepted that cool-flame or autoxidation of hydrocarbons (RH), can produce oxygenated intermediates. It is frequently considered that autoxidation yields ketohydroperoxides (KHPs), the decomposition of which provides chain branching:

$$RH + {}^{\bullet}OH \rightleftarrows R^{\bullet} + H_2O \quad (1)$$

$$R^{\bullet} + O_2 \rightleftarrows ROO^{\bullet} \quad (2)$$

$$ROO^{\bullet} + HOO^{\bullet} \rightleftarrows ROOH + O_2 \quad (3a)$$

$$ROO^{\bullet} + RH \rightleftarrows ROOH + R^{\bullet} \quad (3b)$$

$$ROO^{\bullet} \rightleftarrows {}^{\bullet}QOOH \quad (4a)$$

$$ROO^{\bullet} \rightleftarrows Q\ (\text{unsaturated product}) + HOO^{\bullet} \quad (4b)$$

$${}^{\bullet}QOOH \rightleftarrows {}^{\bullet}OH + QO\ (\text{cyclic ether}) \quad (5)$$

$${}^{\bullet}QOOH + O_2 \rightleftarrows {}^{\bullet}OOQOOH \quad (6)$$

$${}^{\bullet}OOQOOH \rightleftarrows HOO^{\bullet}POOH \rightleftarrows {}^{\bullet}OH + HOOP{=}O\ (\text{KHPs}) \quad (7)$$

$$HOOP{=}O \rightleftarrows {}^{\bullet}OH + OP^{\bullet}O \quad (8)$$

Recently, the production of highly oxidized organic products in cool flames (500–600 K) of alkanes, cycloalkanes, alcohols, aldehydes, ethers, and esters has been reported.[19-21] In this alternative oxidation pathway an H-shift in the ${}^{\bullet}OOQOOH$ intermediate occurs from another H-C group than the H-C-OOH group involved in the formation of KHPs. This mechanism opens new oxidation pathways including a third O_2 addition to $HOOP^{\bullet}OOH$ yielding ${}^{\bullet}OOP(OOH)_2$. This H-shift and O_2 addition sequence can continue further, yielding highly oxidized products.[20-22] Besides, ${}^{\bullet}QOOH$ can decompose to yield radicals and stable products: Reaction (5), ${}^{\bullet}QOOH \rightarrow$ carbonyl product + olefin + ${}^{\bullet}OH$ (9), and ${}^{\bullet}QOOH \rightarrow HO_2^{\bullet}$ + olefin (10). If the initial reactant contains a carbon-carbon double bond, the Waddington mechanism[23] can occur. It involves OH addition to the C=C double bond followed by O_2 addition and H-shift from the –OH group to the $–OO^{\bullet}$ peroxy group, and decomposition:

$$R\text{-}C{=}C\text{-}R' + {}^{\bullet}OH \rightleftarrows R\text{-}{}^{\bullet}C\text{-}C(\text{-}R')\text{-}OH \quad (11)$$

$${}^{\bullet}C(\text{-}R)\text{-}C(\text{-}R')\text{-}OH + O_2 \rightleftarrows {}^{\bullet}OO\text{-}C(\text{-}R)\text{-}C(\text{-}R')\text{-}OH \quad (12)$$

$${}^{\bullet}OO\text{-}C(\text{-}R)\text{-}C(\text{-}R')\text{-}OH \rightleftarrows HOO\text{-}C(\text{-}R)\text{-}C(R')\text{-}O^{\bullet} \quad (13)$$

$$HOO\text{-}C(\text{-}R)\text{-}C(R')\text{-}O^{\bullet} \rightarrow {}^{\bullet}OH + R\text{-}C{=}O + R'\text{-}C{=}O \quad (14)$$

The hydroxyl radical initially consumed is finally regenerated at the end of that reaction scheme. Also, as demonstrated initially in the liquid phase, the Korcek mechanism[24-25] which transforms γ-ketohydroperoxides into a carboxylic acid and a ketone or an aldehyde can occur. The production of these chemicals via the Korcek mechanism has been suggested to happen under atmospheric conditions[26] and has also been introduced in recently proposed combustion kinetic reaction mechanisms.[27-28] Further evidence of the occurrence of that mechanism has been presented recently.[29]

This study aims to better characterize the autoxidation products of limonene under cool-flame conditions. Thus, we performed oxidation experiments of limonene-O_2-N_2 mixtures in a JSR at 1 bar, an equivalence ratio, φ, of 0.5, and over a range of temperatures (520-800 K). We used online Fourier transform infrared (FTIR) spectroscopy for quantifying simple products. Orbitrap Q-Exactive® analyses were performed with ultra-high-performance liquid chromatography (UHPLC) and flow-injection (FIA). 2,4-dinitrophenyl hydrazine (2,4-DNPH) derivatization of carbonyls and H/D exchange were used to characterize the oxidation products dissolved in acetonitrile (ACN).

2. METHODS

2.1 JSR. Experiments were conducted in a fused silica JSR (42 mL) introduced earlier.[30] As previously[31-32] limonene (R)-(+) ($C_{10}H_{16}$, >97%, Sigma-Aldrich®) was pumped using a HPLC pump with an online degasser (LC10 AD VP and DGU-20 from Shimadzu, respectively). The fuel was delivered to a vaporizer assembly fed with a flow of nitrogen (N_2). Limonene-N_2 and oxygen-N_2 flowed separately to the JSR to avoid premature oxidation before reaching the reactor. The flow rates of N_2 and O_2 were delivered by mass flow meters. Thin thermocouples (0.1 mm Pt-Pt/Rh-10% wires located inside a thin-wall silica tube) were moved along the vertical axis of the JSR to verify good thermal homogeneity (gradients of < 1 K/cm). For observing the oxidation of limonene, which is relatively unreactive in the cool-flame regime, we oxidized 1% limonene at 1 bar, in excess of oxygen (φ = 0.5, 28% O_2, 71% N_2), at a residence time of 1.5 s, and over the temperature range 520-800 K. Under these conditions, the oxidation of limonene is initiated via H-atom abstraction by O_2. Fuel radicals readily react with O_2, producing peroxy radicals which undergo further oxidation. Besides, oxidation can proceed through the Waddington and Korcek mechanisms, as presented in the previous Section.

2.2 Chemical analyzes. Gas samples were taken using a low-pressure sonic probe connected to a FTIR spectrometer (Nexus 470 from Nicolet). The FTIR gas cell conditions were as follows: pathlength = 10 m, pressure = 200 mbar, and controlled temperature = 145°C. Standards were used for calibrating the FTIR. Due to the complexity of the composition of the reacting mixture, the infrared measurements of CO_2 mole fractions present uncertainties higher than the usual 10-20 %. Nevertheless, we checked carefully the validity of the mole fractions extracted from the different recordings using the OMNIC and QuantPad softwares (ThermoScientific) and confirm the error bars presented in Fig. 1. In addition, low-temperature oxidation products ranging from ketohydroperoxides (KHPs) to highly oxidized products (HOPs), were collected by bubbling gas samples for 60 min, taken over a reduced temperature range of

540-680 K, into 20 mL of UHPLC grade ≥99.9 acetonitrile held at 0°C. These samples were kept in a freezer at -15°C for future chemical analyses. We could see no significant degradation of the fragile products, such as ROOH and HOPs, after few weeks of storage. Analyzes were conducted by flow injection analyses/heated electrospray ionization (FIA/HESI). The HESI settings were as follows: sheath gas = 15 arbitrary units (a.u.), auxiliary gas flow = 1 a.u., vaporizer temperature = 120°C, capillary transfer temperature = 300°C, spray voltage = 4.2 kV, flow injection = 5 µL/min. Ionization signals were recorded for 1 min for averaging. The samples were analyzed by high-resolution mass spectrometry (HRMS). We used an Orbitrap Q-Exactive® (Thermo Scientific™) with mass accuracy <0.5 ppm RMS and mass resolution of 140,000. We performed mass calibrations in positive and negative modes by injecting +/– HESI Pierce™ calibration mixtures (Thermo Scientific). Unfortunately, no standard is available commercially for several of the low-temperature oxidation products. Reverse-phase ultra-high-performance liquid chromatography (RP-UHPLC) analyses were conducted using a C_{18} analytical column (Phenomenex Luna, 1.6µm, 100 Å, 100x2.1 mm). The column was located in a temperature-controlled oven maintained at 40°C. 3 µL of samples were eluted by water-ACN mix at a flow rate of 250 µL/min (gradient 5% to 90% ACN, during 33 min). Atmospheric pressure chemical ionization (APCI) was used in positive and negative modes for the ionization of products. APCI settings were as follows: vaporizer temperature = 120°C, capillary transfer temperature = 300°C, sheath gas flow = 50 a.u., auxiliary gas flow = 3 a.u., sweep gas flow = 0 a.u., corona discharge current = 5 µA. Injecting of a solution of limonene in ACN was used to check that no substantial oxidation occurred in the ion source. The optimization of the Orbitrap APCI parameters did not show any clustering phenomenon under these conditions. For the determination of the chemical structure of oxidation products, MS/MS analyses were conducted at a collision cell energy of 10 eV. As in previous works,[33-34] 2,4-Dinitrophenylhydrazine (2,4-DNPH, $C_6H_6N_4O_4$) was also used to assess the presence of carbonyl compounds. To this end, 100 µL of 2,4-DNPH solution (2 g in 100 mL ACN) and 20 µL of H_3PO_4 (purity 85%) were added to 1 mL of sample. As in previous experimental investigations,[20-21] the fast OH/OD exchange was used to assess to the presence of a hydroxyl (-OH) or hydroperoxyl (-OOH) groups in oxidation products. We added 300 µL of high-purity D_2O (Sigma-Aldrich®) to 1 mL of samples and let the mix react for 20 min. We analyzed that solution using FIA-HESI-HRMS and UHPLC-APCI-HRMS.

3. RESULTS AND DISCUSSION

One percent of limonene was oxidized over the temperature range 520-800 K, atmospheric pressure, $\varphi = 0.5$, and constant residence time (1.5 s). Although the fuel conversion is moderate under these conditions, the production of cool-flame products could be observed. Figure 1 shows the variation of the mole fractions (±10-20%) of simple products measured by FTIR. As can be seen from that figure, the concentrations of several products (CO, CO_2, H_2O, HCOOH, CH_3COOH, and C_2H_4) increased

moderately until ~700 K. Formaldehyde started to accumulate at much lower temperature, as a result of low-temperature chemistry. Above that temperature, their rates of formation increase very significantly. Below 700 K, no clear cool-flame with a negative temperature coefficient region could be observed under the present conditions, likely due to the low cetane number of the fuel.

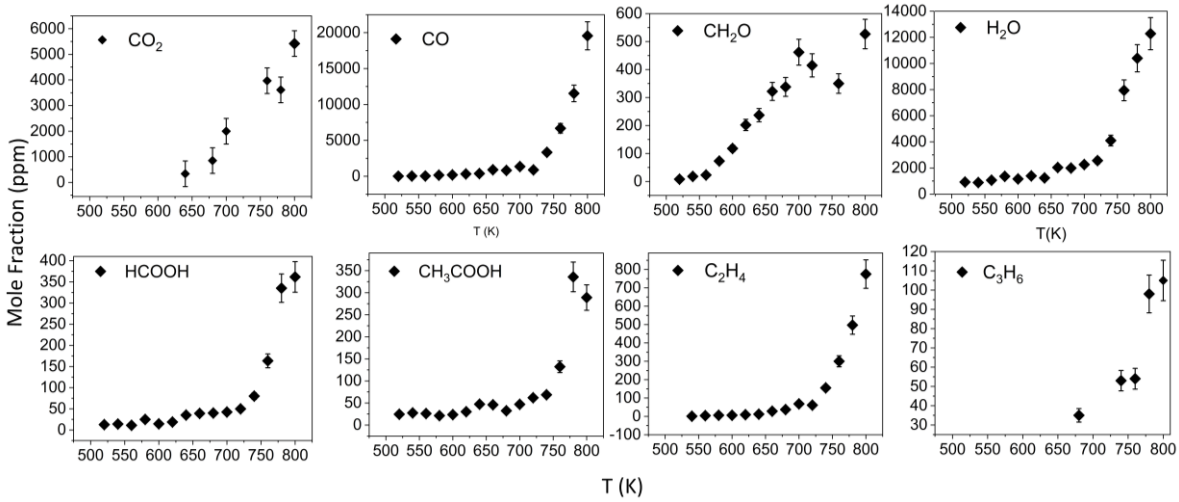

Figure 1. Experimental mole fractions of limonene oxidation products measured online by FTIR.

One can note that formic acid and acetic acid are formed in similar quantities (maximum production of 400 ppm at ~ 780-800 K) whereas they are slightly produced below ~ 700 K (20 to 50 ppm). Ethylene and propene were measured showing similar variation of their mole fractions versus temperature, although those of ethylene reach values ~ 5 times higher than those of propene over the temperature range 520-800 K.

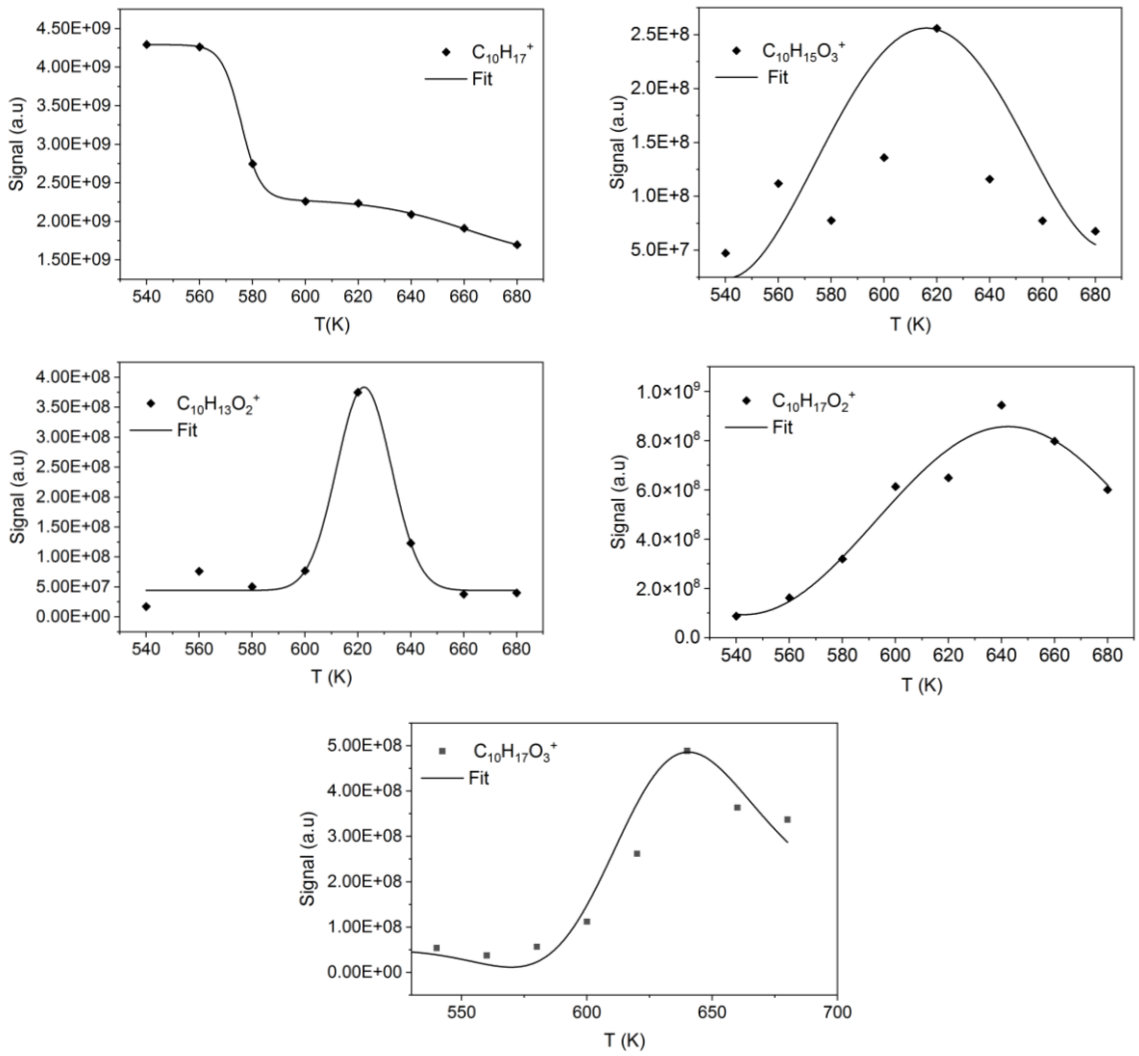

Figure 2. HRMS signal obtained for limonene and products of its oxidation. The data for limonene ($C_{10}H_{16}$), isoprenyl-6-oxoheptanal and isomers ($C_{10}H_{16}O_2$), and limononic acid and isomers ($C_{10}H_{16}O_3$) were obtained after integrating RP-UHPLC-HRMS APCI (+) signal ($C_{10}H_{17}^+$ *m/z* 137.1324; $C_{10}H_{17}O_2^+$ *m/z* 169.1223, and $C_{10}H_{17}O_3^+$ *m/z* 185.1172, respectively). The data for ketohydroperoxides and their isomers ($C_{10}H_{14}O_3$) and diketones and their isomers ($C_{10}H_{12}O_2$) were obtained using FIA and HESI (+), i.e., $C_{10}H_{15}O_3^+$ *m/z* 183.1015 and $C_{10}H_{13}O_2^+$ *m/z* 165.0910, respectively. A 40% error is assumed for these measurements (15% for JSR experiments and 25% for collection and MS measurements), as in previous works.[22] Repeatability tests indicated that our 25% uncertainty for collection and analysis is an upper limit.

Figure 2 shows the variation of the HRMS signals for several products detected in this work as a function of reactor temperature. It is evident that limonene begins to react at temperatures greater than 560 K. Its consumption significantly increases between 560 and 600 K and slows down at higher temperatures. The signals for isoprenyl-6-oxoheptanal ($C_{10}H_{16}O_2$) and limononic acid ($C_{10}H_{16}O_3$) peak

at ~ 640 K, whereas the products of the 2nd addition of O_2 on limonene radicals ($^{\bullet}C_{10}H_{15}$), KHPs ($C_{10}H_{14}O_3$) and diketones ($C_{10}H_{12}O_2$), peak at ~ 620 K.

Besides, products of the first O_2 addition to the fuel radicals were detected. Indeed, hydroperoxides ($C_{10}H_{16}O_2$) formed in reaction (3a) and (3b), and ($C_{10}H_{14}O$) carbonyls or cyclic ethers, the later being formed via reaction (5), were observed. We used the reaction with 2,4-DNPH to differentiate carbonyls from cyclic ethers, which do not react. 100 µL of a 2,4-DNPH solution were introduced into 1 mL of samples. We let reaction proceed for more than 25 hours before analysis. Figure S1 (Supporting Information) shows the results obtained by UHPLC-APCI(+)-MS. At least the intensity of three chromatographic peaks did not change, indicating the absence of C=O groups and the likely presence of cyclic ethers. Hydroperoxides were tracked using H/D exchange with D_2O (see Section 2.2). We could detect the clear presence of $C_{10}H_{15}D_1O_2$ after H/D exchange (Fig. S2, Supporting information) which should correspond to ROOH. Among other products of oxidation, we observed products containing an additional unsaturation ($C_{10}H_{14}$). Indeed, several isomers were detected using UHPLC-APCI(+)-MS (Supporting Information, Fig. S3). They could be formed via H-shift followed by $HO_2^{\bullet}$ elimination (reaction 4b).

3.1 Characterization of KHPs and derived products. KHPs contain C=O and OOH groups. The presence of OOH was probed using H/D exchange with D_2O (see Section 2.2). It was confirmed here (Supporting Information, Table S1). However, a weaker second H/D exchange which could be due to the presence of two OH groups in isomers was observed (Supporting Information, Table S1).

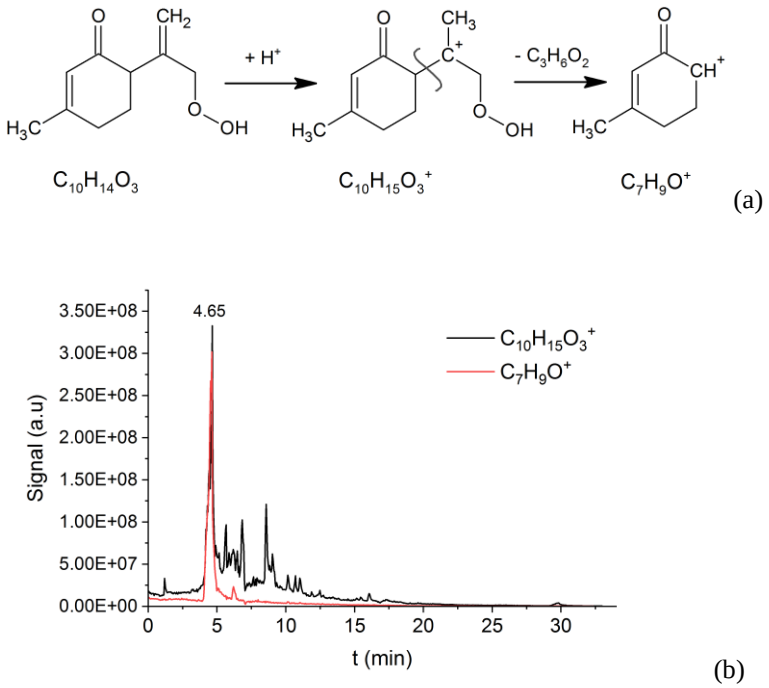

Figure 3. (a) Proposed fragmentation mechanism for the $C_{10}H_{14}O_3$ isomer #6; (b) Chromatograms obtained for $C_{10}H_{14}O_3$ ($C_{10}H_{15}O_3^+$ *m/z* 183.1015) and the fragment $C_7H_9O^+$ (*m/z* 109.0650). Correspondence of the ion signal at ~4.65 min supports the fragmentation mechanism presented in (a).

A MS/MS spectrum is presented in the Supporting Information, Fig. S5a. Note: As here, the APCI(–) MS/MS spectrum of a cumene hydroperoxide standard showed no HOO loss, as expected in negative ionization mode, but a main fragment $C_6H_5O^-$ deriving from the loss of C_3H_6O by the $C_9H_{11}O_2^-$ ions.

To assess the existence of C=O groups in chemical products, 100 µL of a 2,4-DNPH solution were introduced into 1 mL of samples. We let reaction proceed for up to 25 hours before analysis. Chemical characterization was performed by RP-UHPLC-APCI (–)/HRMS, recording *m/z* 361.1153 ($C_{16}H_{17}O_6N_4^-$) from the $C_{16}H_{18}O_6N_4$ KHPs/DNPH derivative: $C_{10}H_{14}O_3 + C_6H_6O_4N_4 \rightleftarrows C_{16}H_{18}O_6N_4 + H_2O$ (15). Several isomers among the structures (Supporting Information, Figure S4) were observed, with longer retention times than those corresponding KHPs. A subset of KHPs formation pathways is presented in Scheme S1a (Supporting Information). Through APCI (+)-MS/MS analysis of the chromatographic peak at ~ 4.65 min (Figure 3), we could confirm the chemical structure of the KHP isomer #6 (Supporting Information, Figure S5). The fragmentation mechanism is shown in Figure 3a and the chromatogram for $C_{10}H_{15}O_3^+$ and the main fragment $C_7H_9O^+$ are presented in Figure 3b showing the perfect match for these two ions.The formation of this isomer is favorable through a 1,6-H transfer leading to the production of KHP #6 (Supporting Information, Figure S5b). When we analyzed limonene oxidation products, we recorded a strong MS signal (1.09E8) for KHPs and isomers ($C_{10}H_{15}O_3^+$) and a lower intensity fragment ($C_{10}H_{13}O^+$ *m/z* = 135.08018) for the loss of H_2O_2 (MS signal =1.79E5) at ~4.65 min. Because this fragment's intensity is low in comparison to those of the $C_{10}H_{15}O_3^+$ and $C_7H_9O^+$ ions, we did not include its profile in Fig. 3 (b). Further MS/MS analyses of the other chromatographic peaks could not confirm the molecular structure of the eluted isomers. One should note that characterizing KHPs is difficult because these chemicals are relatively unstable and decompose via different mechanisms. One of the reactions described in the literature is their spontaneous dehydration to produce diketones via $C_{10}H_{14}O_3 \rightleftarrows C_{10}H_{12}O_2 + H_2O$ (16).[35] Our data confirmed the presence of diketones, $C_{10}H_{12}O_2$, detected both by elution of oxidation products of limonene (chromatographic peaks at 8.54, 10.02, 11.5, and 12.05 min), see Supporting Information (Figure S6), and also present in the chromatographic peaks of KHP isomers. This indicates that spontaneous decomposition of KHPs can occur in the mass spectrometer. Nevertheless, this study proved the formation of KHPs during limonene oxidation.

3.2 Korcek pathway. The Korcek mechanism[25] produces carbonyl compounds (aldehydes or ketones) and carboxylic acids via the decomposition of γ-KHPs. Among the 18 proposed KHPs (Supporting Information, Figure S4), four isomers (#4, 11, 15, and 18) could decompose according to the Korcek mechanism. However, only the isomerization of the #4 KHP isomer (Supporting Information, Figure S4) will likely form a cyclic organic peroxide intermediate between the carbonyl and hydroperoxyl groups. After ring opening, the other three isomers would yield $C_{10}H_{14}O_3$ isomers. For the #4 KHP isomer, the Korcek mechanism yields a carbonyl compound, $C_9H_{12}O$, and formic acid, CH_2O_2 (Scheme 1), both detected in this study (Figure 1 and Table S1).

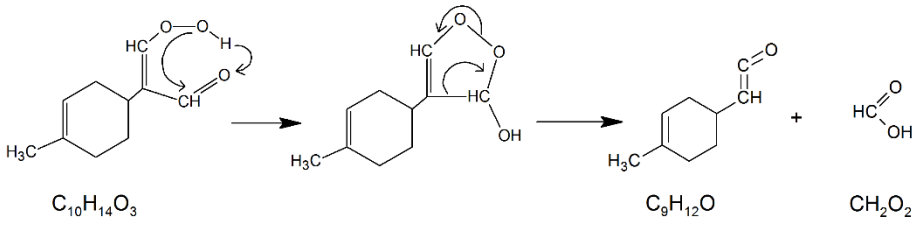

(15)

Scheme 1. Reaction of the #4 ketohydroperoxide isomer according to the Korcek mechanism leading to the formation of $C_9H_{12}O$ and CH_2O_2.

We proposed a fragmentation mechanism for $C_9H_{12}O$ where the fragment $C_7H_{11}^+$ (*m/z* 95.0855) is formed from $C_9H_{13}O^+$, *m/z* 137.0960 (Figure 4a). RP-UHPLC analyses confirmed the presence of six $C_9H_{12}O$ isomeric products chemical formula (Figure 4b). Only the intensity of the chromatographic peak located at 7.02 min decreased strongly after reaction with 2,4- DNPH (Supporting Information, Figure S7), which indicates that only the isomer eluted at 7.02 min contains a carbonyl group. The reaction with the 2,4-DNPH and MS/MS analyses allowed us to characterize this product (Figure 4).

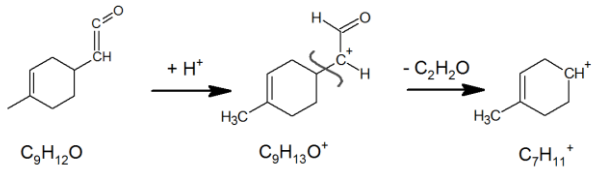

(a)

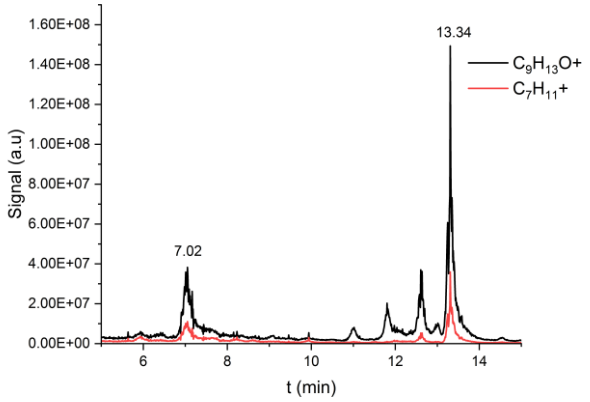

(b)

Figure 4. (a) The proposed fragmentation mechanism for the $C_9H_{12}O$ isomer shown in Scheme 1. (b) Chromatograms obtained for $C_9H_{12}O$ ($C_9H_{13}O^+$ *m/z* 137.0960) and the fragment $C_7H_{11}^+$ (*m/z* 95.0855).

3.3. Other routes to carboxylic acids. Besides the Korcek mechanism, other routes can yield carboxylic acids. As an example, perillic acid ($C_{10}H_{14}O_2$) formation could result from H-atom abstraction on the methyl group of limonene, followed by peroxidation, reaction with a peroxy radical, $ROO^\bullet + R'OO^\bullet \rightarrow RO^\bullet + R'O^\bullet + O_2$ (17), and reaction with O_2 yielding the corresponding aldehyde. In turn, that aldehyde

could oxidize to the corresponding carboxylic acid via the mechanism proposed by Madronich et al.[36] for acetic acid formation from acetaldehyde (Scheme 2). We tracked perillic acid in our samples using a standard and found traces of this product co-eluted with an isomer. Our results indicated that this oxidation route is of minor importance under our experimental conditions.

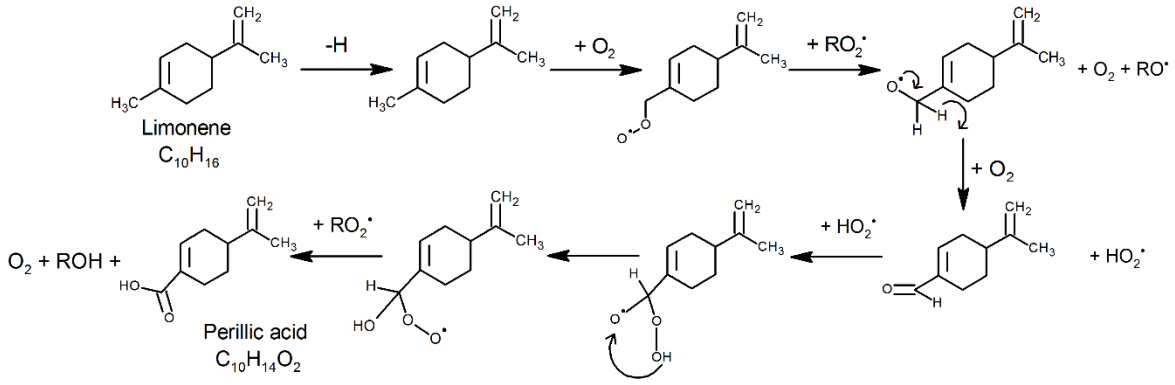

Scheme 2. Proposed formation route for perillic acid during limonene oxidation. The pathway to aldehyde and that to perillic acid have been described previously for other reactants.[36-37]

3.4 Waddington mechanism. We tracked products of the Waddington reaction mechanism[38] using RP-UHPLC-HRMS (Figure 5). This mechanism, through which the oxidation of a C=C group occurs can involve *exo*-cyclic and *endo*-cyclic C=C groups in limonene. The oxidation of the *exo*-cyclic C=C will produce a ketone, $C_9H_{14}O$, and formaldehyde (CH_2O). The oxidation of the *endo*-cyclic C=C yields $C_{10}H_{16}O_2$, isoprenyl-6-oxoheptanal (Scheme 3). As shown in Figure 5, several isomers were characterized by RP-UHPLC-HRMS ($C_9H_{15}O^+$ *m/z* 139.1117, $C_{10}H_{17}O_2^+$ with *m/z* 169.1223). Among them, isoprenyl-6-oxoheptanal was detected at 13.79 min by injecting a standard (Supporting Information Figure S8). The MS/MS spectrum obtained via the fragmentation of products eluted at 13.79 min is exactly the same as that of isoprenyl-6-oxoheptanal, which confirms the presence of this substance in the oxidation products.

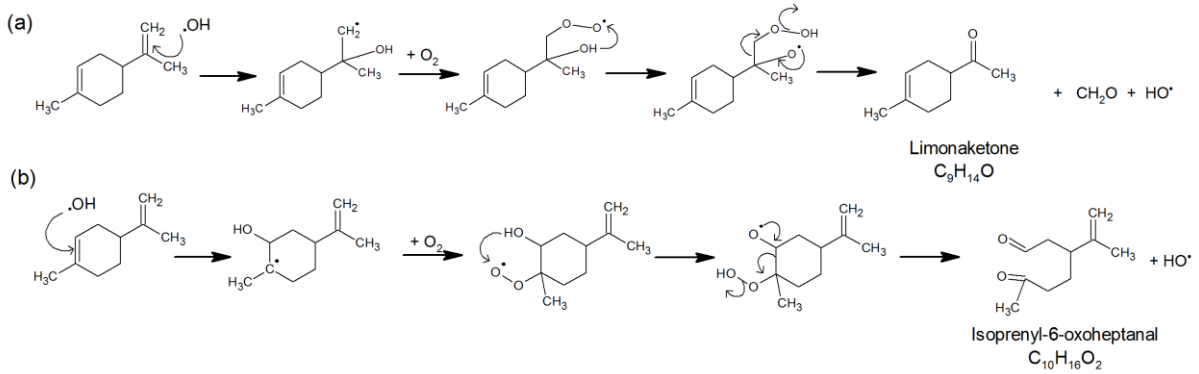

Scheme 3. Oxidation of *exo*- (a) and *endo*-(b) cyclic C=C groups in limonene via the Waddington mechanism.

The fragmentation of these isomers allowed their identification (Supporting Information, Scheme S2, Scheme S3, and Figures S8 and S9). We confirmed the presence of a C=O group by 2,4-DNPH derivatization. RP-UHPLC analyses were performed and APCI in negative mode was used. Only the compounds $C_{16}H_{20}O_5N_4$, $C_{10}H_{16}O_2 + C_6H_6O_4N_4 \rightleftarrows C_{16}H_{20}O_5N_4 + H_2O$ (18), and $C_{15}H_{18}O_4N_4$, $C_9H_{14}O + C_6H_6O_4N_4 \rightleftarrows C_{15}H_{18}O_4N_4 + H_2O$ (19) were detected ($C_{16}H_{19}O_5N_4^-$, *m/z* 347.1360 and $C_{15}H_{17}O_4N_4^-$, *m/z* 317.1255, respectively). The reaction of the second carbonyl group in $C_{10}H_{16}O_2$ should yield $C_{22}H_{24}O_8N_8$ by reaction with 2,4-DNPH. However, the formation of that derivative could not be confirmed here.

We also used D_2O to assess the presence of -OH or -OOH groups through H/D exchange. RP-UHPLC-APCI (+)/HRMS analyses, where water was replaced by D_2O as solvent, indicated the occurrence of H/D exchanges by detecting $C_{10}H_{16}D_1O_2^+$, *m/z* 170.1258, $C_{10}H_{15}D_2O_2^+$ *m/z* 171.1348 for $C_{10}H_{16}O_2$, which may suggest that other isomers, such as diols, are eluted together with isoprenyl-6-oxoheptanal. Additionally, by detecting $C_9H_{14}D_1O^+$ *m/z* 140.1180 in the case of $C_9H_{14}O$ which could indicate that this ketone is eluted simultaneously with an isomer that have an OH group.

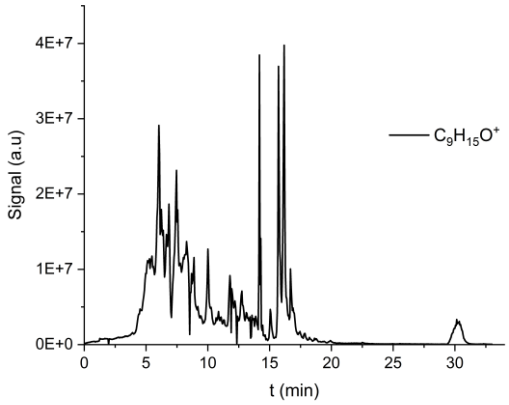

(a)

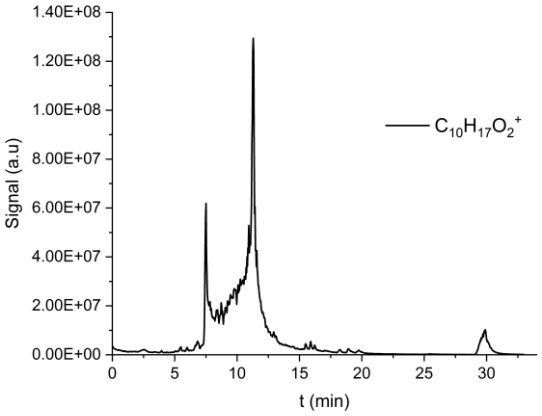

(b)

Figure 5. Chromatograms of (a) $C_9H_{14}O$ ($C_9H_{15}O^+$ *m/z* 139.1117) and (b) $C_{10}H_{16}O_2$ ($C_{10}H_{17}O_2^+$ *m/z* 169.1223) isomers. Analyses were carried out using RP-UHPLC-APCI (+).

In recent kinetic modeling of the Waddington mechanism,[39] it was noted that chemical structure impact the energy barriers associated with the dissociation step. The authors indicated a decrease in the activation energy when the substitution of the C-atom carrying the peroxy group increases. They also reported that this effect is increased by the degree of the substitution of the C-atom carrying the -OH group, which seems in line with the higher signal detected for $C_{10}H_{16}O_2$ which has the most substituted C-atom carrying a peroxy group. Also, it has been demonstrated earlier that the *endo* double bond is more reactive than the *exo* C=C.[40] This seems to be confirmed by the results of the present study because higher signals for $C_{10}H_{16}O_2$ than for $C_9H_{14}O$ were recorded (Figure 5). One of the $C_{10}H_{16}O_2$ isomers, namely isoprenyl-6-oxoheptanal, was identified through the injection of a standard (Supporting Information, Figure S9) as mentioned before. The oxidation of isoprenyl-6-oxoheptanal could proceed through $HO_2^\bullet$ addition on the aldehydic C=O, followed by a reaction with $RO_2^\bullet$ forming two $RO^\bullet$ radicals which, in turn, can react with O_2: $RO^\bullet + O_2 \rightarrow {}^\bullet R_{-H}(=O) + HO_2^\bullet$ (20). This reaction route (Scheme 4) can produce limononic acid ($C_{10}H_{16}O_3$) which was detected in the present work (Figure 2), and reported as a product of oxidation of limonene under tropospheric conditions in the literature.[41-44] The identification of limononic acid is based on its fragmentation spectrum and 2,4-DNPH derivatization (Fig. S10, Supporting Information).

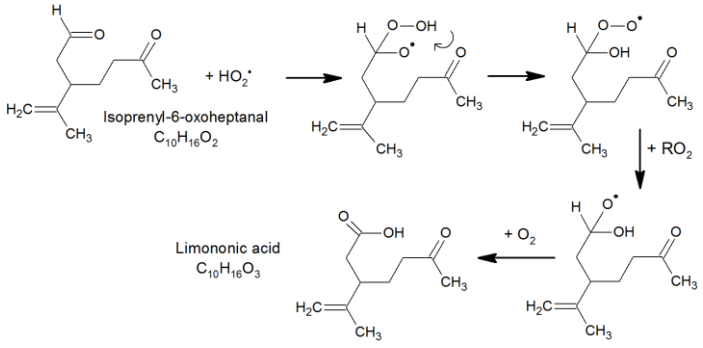

Scheme 4. Proposed pathway for the oxidation of isoprenyl-6-oxoheptanal to limononic acid based on oxidation pathway of aldehydes proposed in the literature[36].

3.5 Formation of highly oxidized products (HOPs) via alternative oxidation pathways. As introduced earlier, KHPs can give rise to branching reactions through the production of hydroxyl radicals.[45] However, if the H-shift in the $^\bullet$OOQOOH intermediate does not concern the H-C-OOH group, but a different H-C group, no KHP is obtained and a 3rd O_2 addition to HOO$^\bullet$POOH can yield $^\bullet$OOP(OOH)$_2$.[20, 34, 46] (Scheme S1b, Supporting Information) If this oxidation path repeats further, it could yield HOPs containing ≥ 5 O-atoms.

Several procedures were considered for tracking the formation of HOPs under the current oxidation experiments. Since the RP-UHPLC separation of isomers is difficult and ion signals are weak,

FIA was selected. Besides KHPs $C_{10}H_{14}O_3$ ($C_{10}H_{15}O_3^+$ *m/z* 183.1015), other odd oxygen-containing species, i.e., $C_{10}H_{14}O_5$ ($C_{10}H_{13}O_5^-$ *m/z* 213.0768), $C_{10}H_{14}O_7$ ($C_{10}H_{13}O_7^-$ *m/z* 245.0666), and $C_{10}H_{14}O_9$ ($C_{10}H_{13}O_9^-$ *m/z* 277.0565) were detected by FIA–HESI–HRMS.

Besides, we also detected even oxygen-containing products such as ketohydroxides and isomers of olefinic hydroperoxides, $C_{10}H_{14}O_2$, ($C_{10}H_{15}O_2^+$ *m/z* 167.1066), which were distinguished using 2,4-DNPH derivatization, as presented in the Supporting Information (Fig. S11). Also, $C_{10}H_{14}O_4$ were detected ($C_{10}H_{15}O_4^+$, *m/z* 199.0964 and $C_{10}H_{13}O_4^-$, *m/z* 197.0819), which may correspond to unsaturated dihydroperoxides and hydroxyl-keto-hydroperoxides. The presence of carbonyl groups in $C_{10}H_{14}O_4$ species was confirmed by 2,4-DNPH derivatization ($C_{16}H_{17}N_4O_7^-$, *m/z* 377.1102). In addition, $C_{10}H_{14}O_6$ isomers were observed during the oxidation of limonene ($C_{10}H_{13}O_6^-$ *m/z* 229.0717). While oxidation products with odd numbers of O-atoms can be formed through autoxidation routes considered in combustion, those with even numbers of O-atoms can derive from alkoxy radicals' reactions proceeding through internal H-shift[47-48] and peroxidation:

$$2\ RO_2^{\bullet} \rightarrow ROOOOR \rightarrow 2\ RO^{\bullet} + O_2 \quad (21)$$

$$RO_2^{\bullet} + HO_2^{\bullet} \rightarrow RO^{\bullet} + {}^{\bullet}OH + O_2 \quad (22)$$

$$RO^{\bullet} \rightarrow {}^{\bullet}R_{\text{-H}}\mathit{OH}\ \text{(H-shift)} \quad (23)$$

$${}^{\bullet}R_{\text{-H}}\mathit{OH} + O_2 \rightarrow {}^{\bullet}OOR_{\text{-H}}\mathit{OH} \quad (24)$$

$${}^{\bullet}OOR_{\text{-H}}\mathit{OH} \rightarrow HOO^{\bullet}R_{\text{-2H}}\mathit{OH} \quad (25)$$

$$HOO^{\bullet}R_{\text{-2H}}\mathit{OH} \rightarrow O{=}R_{\text{-2H}}\mathit{OH} + {}^{\bullet}OH \quad (26)$$

This reaction pathway can continue further (21-24) with H-atom transfer from ${}^{\bullet}OOR_{\text{-H}}\mathit{OH}$ and O_2 addition, followed by sequential H-atom transfer and O_2 addition, yielding HOPs. Products resulting from up to five O_2 additions were observed in the current work (Table S1). We noted a decrease of ion signal with increasing numbers of O-atoms in the oxidation products $C_{10}H_{14}O_{3,5,7,9}$ (~ 5 orders of magnitude; $C_{10}H_{14}O_{3,5,7,9}$ stands for $C_{10}H_{14}O_3$, $C_{10}H_{14}O_5$, $C_{10}H_{14}O_7$, $C_{10}H_{14}O_9$) and $C_{10}H_{14}O_{2,4,6}$ (~ 5 orders of magnitude).

The oxidation of isoprenyl-6-oxoheptanal, formed via the Waddington mechanism (Scheme 4), can proceed through H-atom abstraction of the aldehydic H-atom, followed by third O_2 additions and H-shifts yielding $C_{10}H_{14}O_7$, which was detected in the present work (Scheme 5).

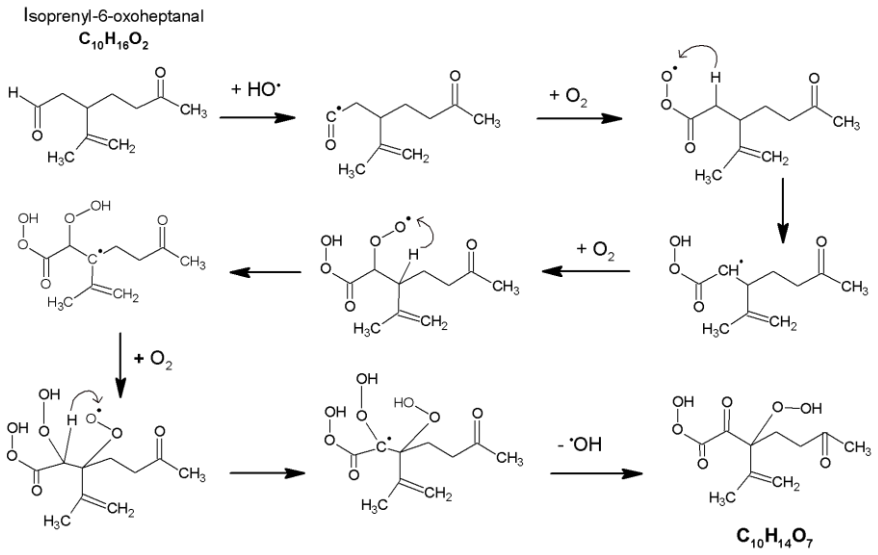

Scheme 5. Formation of $C_{10}H_{14}O_7$ through the oxidation of isoprenyl-6-oxoheptanal.

A large set of oxidation products, with M.W. in the range 136-234 g/mol, was formed during the oxidation of limonene and detected using RP-UHPLC-APCI-HRMS (+/–) analyses, as shown in Table S1 (Supporting Information), such as $C_8H_{12}O_2$, $C_8H_{12}O_4$, $C_8H_{14}O_2$, $C_8H_{14}O_4$, $C_9H_{14}O_3$, $C_9H_{14}O_4$, $C_9H_{14}O_5$, $C_{10}H_{14}O$, $C_{10}H_{16}O_4$, $C_{10}H_{16}O_5$, and $C_{10}H_{18}O_6$.

4. CONCLUSIONS

The oxidation of limonene-O_2-N_2 mixtures was performed in a JSR at 1 bar, for temperatures ranging from 520 to 800 K, under fuel-lean conditions ($\varphi = 0.5$), and short residence time (1.5 s). Several analytical techniques were used to characterize samples of reacting mixtures. They included on-line FTIR quantification and offline HRMS analyzes of samples collected in acetonitrile through bubbling. H/D exchange and reactions with 2,4-DNPH were used to prove the presence of OH or OOH and C=O groups, respectively. In addition, MS/MS analyzes (10 eV) allowed us to characterize some oxidation intermediates by studying their fragments. All these analyses showed that a broad range of oxidation products were formed. They ranged from water to highly oxidized products containing ≥ 5 O-atoms: $C_7H_{10}O_4$, $C_7H_{10}O_5$, $C_8H_{12}O_2$, $C_8H_{12}O_4$, $C_8H_{14}O_2$, $C_8H_{14}O_4$, $C_9H_{12}O$, $C_9H_{14}O$, $C_9H_{14}O_3$, $C_9H_{14}O_4$, $C_9H_{14}O_5$, $C_{10}H_{14}O$, $C_{10}H_{12}O_2$, $C_{10}H_{16}O_2$, $C_{10}H_{16}O_3$, $C_{10}H_{14}O_2$, $C_{10}H_{14}O_3$, $C_{10}H_{14}O_4$, $C_{10}H_{14}O_5$, $C_{10}H_{14}O_6$, $C_{10}H_{14}O_7$, $C_{10}H_{14}O_9$, $C_{10}H_{16}O_4$, $C_{10}H_{16}O_5$, and $C_{10}H_{18}O_6$. Reaction pathways were presented to rationalize the formation of oxidized products. They include autoxidation, the Korcek mechanism, the Waddington mechanism on *exo*- and *endo*-double bonds (C=C) and autoxidation of its products, and autoxidation of $RO^{\bullet}$ radicals. The earlier reported higher reactivity of the *endo* double bond *versus* the *exo* double bond seems to be confirmed here based on the higher ion signal obtained for isoprenyl-6-oxoheptanal ($C_{10}H_{17}O_2^+$) *vs*. that for limonaketone ($C_9H_{15}O^+$). This work demonstrated the complexity of oxidation routes and products in the present chemical system. Our results are expected to help build detailed chemical kinetic reaction schemes for the oxidation of the terpene class of fuel. In order to provide more

useful data for future kinetic modeling, one should quantify the products detected by FIA/UHPLC-Orbitrap. This seems a very challenging task because these products are not commercially available. The thermochemistry of these species and reaction rate constants for their formation and consumption or isomerization need to be computed. Also, it would be useful to consider simpler cyclic hydrocarbons to be able to propose structure-activity relationship (SAR) for the estimation of rate constants for the gas phase reactions of terpenes. The oxidation products observed here will likely be released into the troposphere, potentially increasing the pool of VOCs which, in turn will contribute to particulates formation. The analytical methods and physicochemical techniques of characterization used here could be applied to the characterization of the oxidation of other terpenes and simpler model fuels.

ASSOCIATE CONTENT

Supporting Information: (1) Chromatogram of $C_{10}H_{14}O$ isomers, (2) Chromatogram of $C_{10}H_{16}O_2$ isomers, (3) Chromatogram of $C_{10}H_{14}$ isomers, (4) Chemical structure of keto-hydroperoxide $C_{10}H_{14}O_3$ isomers, (5) Fragmentation of $C_{10}H_{14}O_3$, (6) Chromatogram of $C_{10}H_{12}O_2$ isomers, (7) Chromatograms of $C_9H_{12}O$, (8) Formation of KHPs and HOPs, (9) Proposed fragmentation mechanism for protonated isoprenyl-6-oxoheptanal, (10) Proposed fragmentation mechanism for protonated limonaketone, (11) Chromatogram of $C_{10}H_{16}O_2$ isomers and fragmentation, (12) Chromatogram of $C_9H_{14}O$ isomers and fragmentation, (13) Characterization of limononic acid, (14) Chromatograms of $C_{10}H_{14}O_2$ before and after 2,4-DNPH derivatization, (15) Table of limonene oxidation products (2,4-DNPH derivatization and H/D exchange).

ACKNOWLEDGMENTS

The authors received financial support from CPER and EFRD (PROMESTOCK and APPROPOR-e projects), the French Ministry of Research (MESRI), the Labex CAPRYSSES (ANR-11-LABX-0006) and VOLTAIRE (ANR-10-LABX-100) is gratefully acknowledged.

REFERENCES

1. Seinfeld, J. H.; Pandis, S. N., *Atmospheric Chemistry and Physics: From Air Pollution to Climate Change*. 2nd ed.; Wiley-Interscience: Hoboken, NJ, 2006; p 1232.
2. Llusia`, J.; Penuelas, J., Seasonal patterns of terpene content and emission from seven Mediterranean woody species in field conditions. *American Journal of Botany* **2000,** *87*, 133-140.
3. Pourbafrani, M.; Forgács, G.; Horváth, I. S.; Niklasson, C.; Taherzadeh, M. J., Production of biofuels, limonene and pectin from citrus wastes. *Bioresour. Technol.* **2010,** *101*, 4246-4250.
4. Meylemans, H. A.; Quintana, R. L.; Harvey, B. G., Efficient conversion of pure and mixed terpene feedstocks to high density fuels. *Fuel* **2012,** *97*, 560-568.
5. Harvey, B. G.; Wright, M. E.; Quintana, R. L., High-Density Renewable Fuels Based on the Selective Dimerization of Pinenes. *Energy Fuels* **2010,** *24*, 267-273.
6. Harvey, B. G.; Merriman, W. W.; Koontz, T. A., High-Density Renewable Diesel and Jet Fuels Prepared from Multicyclic Sesquiterpanes and a 1-Hexene-Derived Synthetic Paraffinic Kerosene. *Energy Fuels* **2015,** *29*, 2431-2436.

7. Yanowitz, J.; Ratcliff, M. A.; McCormick, R. L.; Taylor, J. D.; Murphy, M. J. *Compendium of Experimental Cetane Numbers*; NREL/TP-5400-67585; National Renewable Energy Lab. (NREL): Golden, CO, 2017.
8. Berndt, T.; Richters, S.; Kaethner, R.; Voigtlaender, J.; Stratmann, F.; Sipilae, M.; Kulmala, M.; Herrmann, H., Gas-phase ozonolysis of cycloalkenes: Formation of highly oxidized RO2 radicals and their reactions with NO, NO2, SO2, and other RO2 adicals. *J. Phys. Chem. A* **2015,** *119*, 10336.
9. Chetehouna, K.; Courty, L.; Mounaim-Rousselle, C.; Halter, F.; Garo, J.-P., Combustion Characteristics of p-Cymene Possibly Involved in Accelerating Forest Fires. *Combust. Sci. Technol.* **2013,** *185*, 1295-1305.
10. Courty, L.; Chetehouna, K.; Chen, Z.; Halter, F.; Mounaim-Rousselle, C.; Garo, J.-P., Determination of laminar burning speeds and markstein lengths of p-cymene/air mixtures using three models. *Combust. Sci. Technol.* **2014,** *186*, 490-503.
11. Courty, L.; Chetehouna, K.; Halter, F.; Foucher, F.; Garo, J.-P.; Mounaim-Rousselle, C., Flame speeds of alpha-pinene/air and limonene/air mixtures involved in accelerating forest fires. *Combust. Sci. Technol.* **2012,** *184*, 1397-1411.
12. Mack, J. H.; Rapp, V. H.; Broeckelmann, M.; Lee, T. S.; Dibble, R. W., Investigation of biofuels from microorganism metabolism for use as anti-knock additives. *Fuel* **2014,** *117*, 939-943.
13. Wallington, T. J.; Dagaut, P.; Kurylo, M. J., Ultraviolet-Absorption Cross-Sections and Reaction-Kinetics and Mechanisms for Peroxy-Radicals in the Gas-Phase. *Chemical Reviews* **1992,** *92*, 667-710.
14. Benson, S. W., The kinetics and thermochemistry of chemical oxidation with application to combustion and flames. *Prog. Energy Combust. Sci.* **1981,** *7*, 125-134.
15. Cox, R. A.; Cole, J. A., Chemical aspects of the autoignition of hydrocarbon-air mixtures. *Combust. Flame* **1985,** *60*, 109-123.
16. Morley, C., A Fundamentally Based Correlation Between Alkane Structure and Octane Number. *Combust. Sci. Technol.* **1987,** *55*, 115-123.
17. Wang, Z. D.; Herbinet, O.; Hansen, N.; Battin-Leclerc, F., Exploring hydroperoxides in combustion: History, recent advances and perspectives. *Prog. Energy Combust. Sci.* **2019,** *73*, 132-181.
18. Zador, J.; Taatjes, C. A.; Fernandes, R. X., Kinetics of elementary reactions in low-temperature autoignition chemistry. *Prog. Energy Combust. Sci.* **2011,** *37*, 371-421.
19. Wang, Z. D.; Chen, B. J.; Moshammer, K.; Popolan-Vaida, D. M.; Sioud, S.; Shankar, V. S. B.; Vuilleumier, D.; Tao, T.; Ruwe, L.; Brauer, E., et al., n-Heptane cool flame chemistry: Unraveling intermediate species measured in a stirred reactor and motored engine. *Combust. Flame* **2018,** *187*, 199-216.
20. Wang, Z.; Popolan-Vaida, D. M.; Chen, B.; Moshammer, K.; Mohamed, S. Y.; Wang, H.; Sioud, S.; Raji, M. A.; Kohse-Höinghaus, K.; Hansen, N., et al., Unraveling the structure and chemical mechanisms of highly oxygenated intermediates in oxidation of organic compounds. *Proceedings of the National Academy of Sciences* **2017,** *114*, 13102-13107.
21. Belhadj, N.; Benoit, R.; Dagaut, P.; Lailliau, M.; Serinyel, Z.; Dayma, G.; Khaled, F.; Moreau, B.; Foucher, F., Oxidation of di-n-butyl ether: Experimental characterization of low-temperature products in JSR and RCM. *Combust. Flame* **2020,** *222*, 133-144.
22. Belhadj, N.; Benoit, R.; Dagaut, P.; Lailliau, M.; Serinyel, Z.; Dayma, G., Oxidation of di-n-propyl ether: Characterization of low-temperature products. *Proc. Combust. Inst.* **2021,** *38*, 337-344.
23. Ray, D. J. M.; Redfearn, A.; Waddington, D. J., Gas-phase oxidation of alkenes: decomposition of hydroxy-substituted peroxyl radicals. *Journal of the Chemical Society, Perkin Transactions 2* **1973**, 540-543.
24. Jensen, R. K.; Korcek, S.; Mahoney, L. R.; Zinbo, M., Liquid-phase autoxidation of organic-compounds at elevated-temperatures .2. Kinetics and mechanisms of the formation of cleavage products in normal-hexadecane autoxidation. *J. Am. Chem. Soc.* **1981,** *103*, 1742-1749.
25. Jalan, A.; Alecu, I. M.; Meana-Paneda, R.; Aguilera-Iparraguirre, J.; Yang, K. R.; Merchant, S. S.; Truhlar, D. G.; Green, W. H., New Pathways for Formation of Acids and Carbonyl Products in Low-Temperature Oxidation: The Korcek Decomposition of gamma-Ketohydroperoxides. *J. Am. Chem. Soc.* **2013,** *135*, 11100-11114.

26. Mutzel, A.; Poulain, L.; Berndt, T.; Iinuma, Y.; Rodigast, M.; Böge, O.; Richters, S.; Spindler, G.; Sipilä, M.; Jokinen, T., et al., Highly Oxidized Multifunctional Organic Compounds Observed in Tropospheric Particles: A Field and Laboratory Study. *Environmental Science & Technology* **2015,** *49*, 7754-7761.
27. Ranzi, E.; Cavallotti, C.; Cuoci, A.; Frassoldati, A.; Pelucchi, M.; Faravelli, T., New reaction classes in the kinetic modeling of low temperature oxidation of n-alkanes. *Combust. Flame* **2015,** *162*, 1679-1691.
28. Xie, C.; Lailliau, M.; Issayev, G.; Xu, Q.; Chen, W.; Dagaut, P.; Farooq, A.; Sarathy, S. M.; Wei, L.; Wang, Z., Revisiting low temperature oxidation chemistry of n-heptane. *Combust. Flame* **2022,** *242*, 112177.
29. Popolan-Vaida, D. M.; Eskola, A. J.; Rotavera, B.; Lockyear, J. F.; Wang, Z. D.; Sarathy, S. M.; Caravan, R. L.; Zador, J.; Sheps, L.; Lucassen, A., et al., Formation of Organic Acids and Carbonyl Compounds in n-Butane Oxidation via gamma-Ketohydroperoxide Decomposition. *Angewandte Chemie-International Edition* **2022,** *61*, 9168-9168.
30. Dagaut, P.; Cathonnet, M.; Rouan, J. P.; Foulatier, R.; Quilgars, A.; Boettner, J. C.; Gaillard, F.; James, H., A Jet-Stirred Reactor for Kinetic-Studies of Homogeneous Gas-Phase Reactions at Pressures up to 10-Atmospheres (~ 1 MPa). *Journal of Physics E-Scientific Instruments* **1986,** *19*, 207-209.
31. Thion, S.; Togbe, C.; Serinyel, Z.; Dayma, G.; Dagaut, P., A chemical kinetic study of the oxidation of dibutyl-ether in a jet-stirred reactor. *Combust. Flame* **2017,** *185*, 4-15.
32. Dayma, G.; Togbe, C.; Dagaut, P., Experimental and Detailed Kinetic Modeling Study of Isoamyl Alcohol (Isopentanol) Oxidation in a Jet-Stirred Reactor at Elevated Pressure. *Energy Fuels* **2011,** *25*, 4986-4998.
33. Belhadj, N.; Lailliau, M.; Benoit, R.; Dagaut, P., Experimental and kinetic modeling study of n-hexane oxidation. Detection of complex low-temperature products using high-resolution mass spectrometry. *Combust. Flame* **2021,** *233*, 111581.
34. Belhadj, N.; Lailliau, M.; Benoit, R.; Dagaut, P., Towards a Comprehensive Characterization of the Low-Temperature Autoxidation of Di-n-Butyl Ether. *Molecules* **2021,** *26*, 7174.
35. Herbinet, O.; Husson, B.; Serinyel, Z.; Cord, M.; Warth, V.; Fournet, R.; Glaude, P.-A.; Sirjean, B.; Battin-Leclerc, F.; Wang, Z., et al., Experimental and modeling investigation of the low-temperature oxidation of n-heptane. *Combustion and flame* **2012,** *159*, 3455-3471.
36. Madronich, S.; Chatfield, R. B.; Calvert, J. G.; Moortgat, G. K.; Veyret, B.; Lesclaux, R., A photochemical origin of acetic acid in the troposphere. *Geophys. Res. Lett.* **1990,** *17*, 2361-2364.
37. Wang, Z.; Ehn, M.; Rissanen, M. P.; Garmash, O.; Quéléver, L.; Xing, L.; Monge-Palacios, M.; Rantala, P.; Donahue, N. M.; Berndt, T., et al., Efficient alkane oxidation under combustion engine and atmospheric conditions. *Communications Chemistry* **2021,** *4*, 18.
38. Li, Y.; Zhao, Q.; Zhang, Y.; Huang, Z.; Sarathy, S. M., A Systematic Theoretical Kinetics Analysis for the Waddington Mechanism in the Low-Temperature Oxidation of Butene and Butanol Isomers. *The Journal of Physical Chemistry A* **2020,** *124*, 5646-5656.
39. Lizardo-Huerta, J. C.; Sirjean, B.; Bounaceur, R.; Fournet, R., Intramolecular effects on the kinetics of unimolecular reactions of β-HOROO˙ and HOQ˙OOH radicals. *Physical Chemistry Chemical Physics* **2016,** *18*, 12231-12251.
40. Witkowski, B.; Al-sharafi, M.; Gierczak, T., Kinetics of Limonene Secondary Organic Aerosol Oxidation in the Aqueous Phase. *Environmental Science & Technology* **2018,** *52*, 11583-11590.
41. Witkowski, B.; Gierczak, T., Characterization of the limonene oxidation products with liquid chromatography coupled to the tandem mass spectrometry. *Atmos. Environ.* **2017,** *154*, 297-307.
42. Bateman, A. P.; Nizkorodov, S. A.; Laskin, J.; Laskin, A., Time-resolved molecular characterization of limonene/ozone aerosol using high-resolution electrospray ionization mass spectrometry. *Phys. Chem. Chem. Phys.* **2009,** *11*, 7931-7942.
43. Tomaz, S.; Wang, D.; Zabalegui, N.; Li, D.; Lamkaddam, H.; Bachmeier, F.; Vogel, A.; Monge, M. E.; Perrier, S.; Baltensperger, U., et al., Structures and reactivity of peroxy radicals and dimeric products revealed by online tandem mass spectrometry. *Nature Communications* **2021,** *12*, 300.

44. Walser, M. L.; Desyaterik, Y.; Laskin, J.; Laskin, A.; Nizkorodov, S. A., High-resolution mass spectrometric analysis of secondary organic aerosol produced by ozonation of limonene. *Phys. Chem. Chem. Phys.* **2008,** *10*, 1009-1022.
45. Wang; Zhandong; Zhang, L.; Moshammer, K.; Shankar, V. S. B.; Lucassen, A.; Hemken, C.; Taatjes, C. A.; Leone, S. R.; Kohse-Höinghaus, K., et al., Additional chain-branching pathways in the low-temperature oxidation of branched alkanes. *Combustion and Flame* **2016,** *164*, 386-396.
46. Belhadj, N.; Benoit, R.; Dagaut, P.; Lailliau, M., Experimental characterization of n-heptane low-temperature oxidation products including keto-hydroperoxides and highly oxygenated organic molecules (HOMs). *Combust. Flame* **2021,** *224*, 83-93.
47. Baldwin, A. C.; Golden, D. M., Alkoxy Radical Reactions - Isomerization of N-Butoxy Radicals Generated from Pyrolysis of N-Butyl Nitrite. *Chem. Phys. Lett.* **1978,** *60*, 108-111.
48. Atkinson, R.; Carter, W. P. L., Reactions of alkoxy radicals under atmospheric conditions: The relative importance of decomposition versus reaction with O2. *J. Atmos. Chem.* **1991,** *13*, 195-210.

TOC graphic

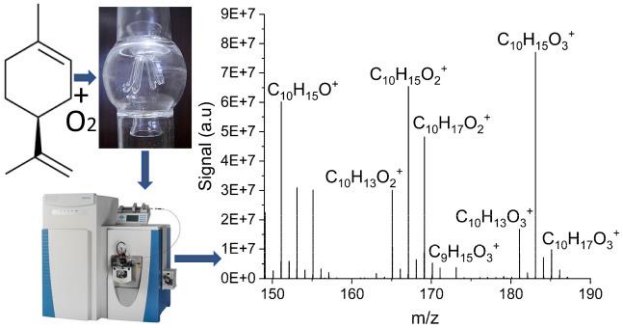
O2
Signal (a.u)
9E+7
8E+7
7E+7
6E+7
5E+7
4E+7
3E+7
2E+7
1E+7
0E+0
150
160
170
180
190
m/z
C10H15O+
C10H15O2+
C10H17O2+
C10H13O2+
C10H15O3+
C10H13O3+
C10H17O3+
C9H15O3+